The Organic Secondary Building Unit: Strong Intermolecular π-Interactions Define Topology in MIT-25, a Mesoporous MOF with Proton-Replete Channels

Sarah S. Park,[1] Christopher H. Hendon,[1] Alistair J. Fielding,[2] Aron Walsh,[3,4] Michael O'Keeffe[5] and Mircea Dincă[1*]

[1] Department of Chemistry, Massachusetts Institute of Technology, 77 Massachusetts Avenue, Cambridge, MA 02139, United States

[2] School of Chemistry and the Photon Science Institute, The University of Manchester, Manchester, M13 9PL, United Kingdom

[3] Department of Materials, Imperial College London, London, SW7 2AZ, United Kingdom

[4] Department of Materials Science and Engineering, Yonsei University, Seoul, South Korea

[5] School of Molecular Sciences, Arizona State University, Tempe, Arizona, 85287, United States

Supporting Information Placeholder

ABSTRACT: The structure-directing role of the inorganic secondary building unit (SBU) is key for determining the topology of metal-organic frameworks (MOFs). Here, we show that organic building units relying on strong π interactions that are energetically competitive with the formation of common inorganic SBUs, and can play a role in defining topology. We demonstrate the importance of the organic SBU in the formation of $Mg_2H_6(H_3O)(TTFTB)_3$, a mesoporous MOF with the new **ssp** topology. A delocalized electronic hole is critical in the stabilization of the TTF triad organic SBUs and exemplifies a design principle for future MOF synthesis.

The topology of a metal-organic framework (MOF) is dictated by the geometries of both the inorganic secondary building units (SBUs) and the ligands. Predicting topology by combining SBUs and ligands with predefined geometry is a feature of reticular chemistry.[1] It has allowed the synthesis of thousands of new materials with increasingly complex topologies even though the experimental conditions that lead to the self-assembly of a given inorganic SBU are largely empirical. The premise of reticular chemistry is that most common SBUs are thermodynamic sinks whose formation and structure are rarely disturbed by non-covalent interactions. However, because reticular chemistry relies on strong, directional bonding between ligands and metals/metal clusters, its predictions break down when non-covalent interactions compete energetically with coordination bonds. This results in surprising and often new topologies.

We have set out to learn whether we can predict when thermodynamic products are likely to deviate from those predicted by reticular chemistry and what are the causes that lead to these exceptions. We further ventured to test whether the non-covalent interactions that prevent the formation of empirically expected SBUs may be used to direct topology themselves. This would provide access to new materials and contribute to a deeper understanding of the physical principles governing MOF synthesis.

Here, we report the synthesis and characterization of a new three-dimensionally connected MOF, $Mg_2H_6(H_3O)(TTFTB)_3$ (TTFTB = tetrathiafulvalene-tetrabenzoate), denoted as **MIT-25**, whose topology is defined by strong intermolecular π– and hydrogen bonding interactions. **MIT-25** exhibits permanent 26.4 × 30.5 Å mesopores running parallel to smaller pores occluded by hydronium ions. Controlling topology by employing π-stacked organic supramolecular building blocks[2] (i.e. organic secondary building units) serves as a powerful paradigm for the design of novel hybrid frameworks.

In some cases, π interactions provide a stablization energy of at least -13.0 kcal/mol,[3] far greater than hydrogen bonding in water (1-6 kcal/mol depending on the conditions),[4] and competitive with even some metal-ligand bonds[5] frequently found in MOFs. It is therefore conceivable that using ligands with a high propensity for π stacking will be competitive with formation of canonical inorganic SBUs, leading to the formation of unusual topologies centered around the π-stacked organic SBUs. Hints of strong π interactions influencing topology in MOFs came from previous work with H_4TTFTB, which formed unusual helical stacks of TTF within frameworks made with transition metals.[6] We reasoned that reacting this ligand with metals exhibiting even more ionic (*i.e.* weaker) M–O bonds, such as Mg^{2+},[5] would promote the isolation of topologies where organic SBUs play more prominent roles.

Reaction of H_4TTFTB with $Mg(NO_3)_2{\cdot}6H_2O$ in a mixture of *N*,*N*-diethylformamide (DMF), water, and ethanol yielded red needles of $Mg_2H_6(H_3O)(TTFTB)_3{\cdot}(DMF)_{1.5}(H_2O)$, which crystallizes in space group $R\bar{3}$ (Figure 1a). Three TTFTB ligands form a tightly packed organic secondary building unit with TTF···TTF distances of 3.73 Å. These triad organic SBUs do not form an infinitely continuous intermolecular π-stacks, but exhibit close intertriad S···S contacts of 3.56 Å (Figure 1b and e). The twelve carboxylates in each triad are connected to four Mg^{2+} ions, and each octahedral Mg^{2+} ion is connected facially to two independent triads. Although individual Mg^{2+} ions are separated by at least 10.23 Å, thereby forming monometallic inorganic SBUs, the coordination environment around each Mg^{2+} ion is further supported by three μ_2-protons that are shared between neighboring carboxylates on the same Mg^{2+} ion (Figure 1c).

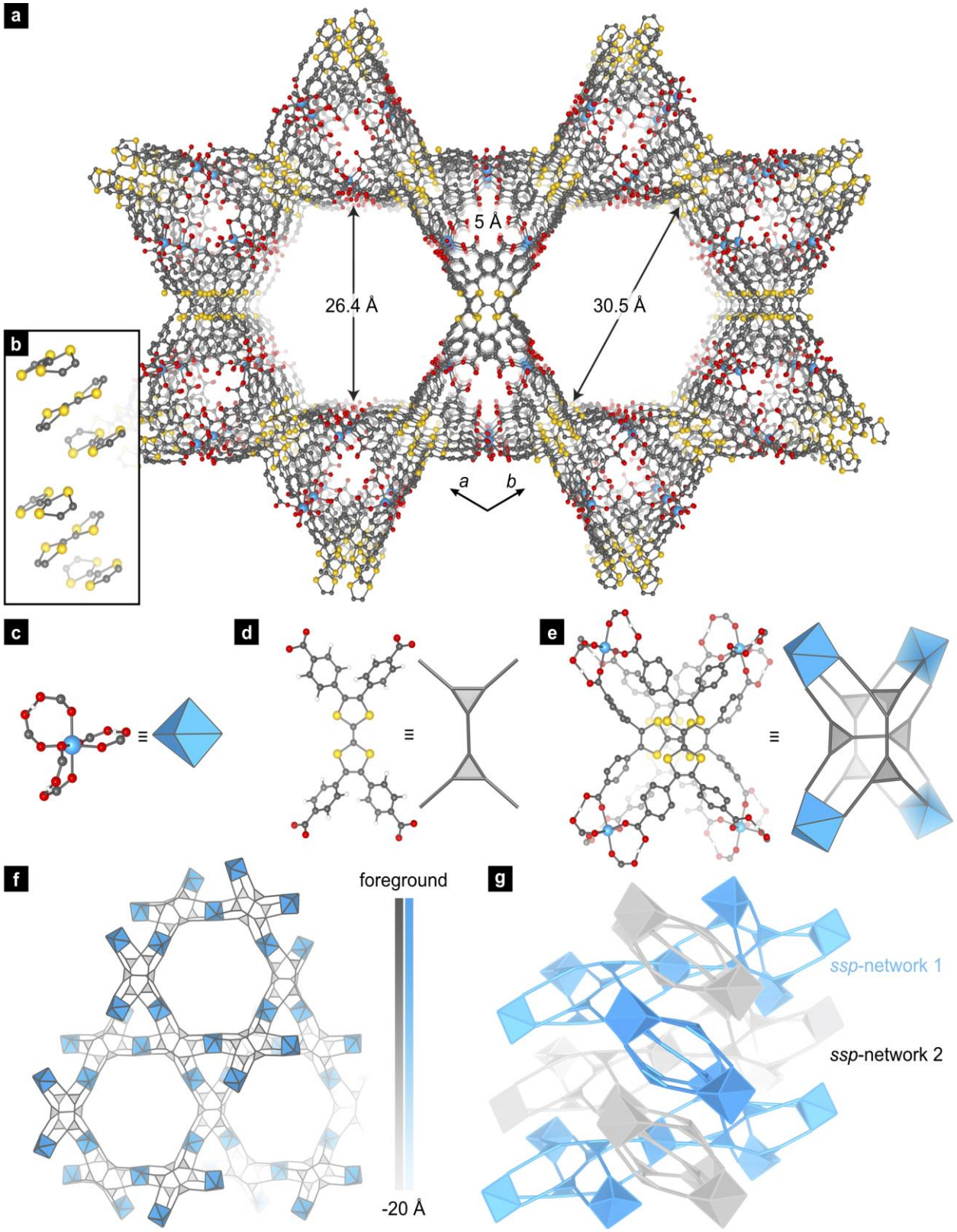

Figure 1. (a) A portion of the X-ray crystal structure of **MIT-25** featuring distinct mesopores. (b) The walls are constructed from TTF trimeric stacks aligned along the *c* axis. (c) The structure exhibits a mononuclear octahedral Mg^{2+} inorganic SBU supported by three additional protons that bridge pairs of carboxylate groups. (d) Ligand and metal nodes are represented by grey and blue shapes, respectively. (e) Four neighboring Mg^{2+} sites are linked by a TTFTB triad. (f) A representation of a single **ssp** net within **MIT-25**, exhibiting a 'three-tier' hexagonal pore structure. (g) The small pore is helical, and the **ssp** net allows interpenetration of two densely woven frameworks, forming the terminal TTF stacks in the *c*-direction.

The crystallographic positions of these shared protons could not be determined from X-ray diffraction analysis alone. Their position bridging between two oxygen atoms was assigned from density functional theory (DFT) calculations (Figure 1c). This unusual inorganic SBU was further explored by construction of a cluster model, $[Mg(OAc)_6H_3]^-$ shown in Figure S1, which upon geometric relaxation converged to a tri-μ_2-H^+ conformation analogous to that observed in **MIT-25**. Importantly, omission of the μ_2 protons in this model system resulted in the destruction of the octahedral coordination environment, inferring that the protons serve both charge-balancing and structural roles.

Considering each TTFTB ligand as two three-connected nodes (Figure 1d), and each $MgH_3(O_2C–)_6$ unit as a six-connected node (Figure 1c), **MIT-25** self-assembles into the new **ssp** topology (a 3,3,6-connected net, Figure 1f). The **ssp** topology is most closely related to the **nbo** net (a comparison is presented in Figure S2). In **MIT-25**, two **ssp** nets are interpenetrated (Figure 1g) and define two parallel channels in the *c* axis with geometric pore apertures of 26.4 × 30.5 Å and 5.0 × 5.6 Å (Figures 1a and S3).

MIT-25 is permanently mesoporous. Thermogravimetric analysis of **MIT-25** upon washing with DMF and ethanol, followed by a 2-day soaking in tetrahydrofuran (THF) revealed a plateau between approximately 100 and 200 °C (Figure S4). Heating a sample of **MIT-25** under vacuum at 200 °C followed by an N_2 adsorption isotherm at 77 K revealed a Type IV isotherm with a maximal N_2 uptake of ~330 cm^3/g. Barrett-Joyner-Halenda (BJH) pore size analysis[7] using Kruk-Jaroniec-Sayari correction[8] for hexagonal pores and Brunauer-Emmett-Teller (BET)[9] fits to this isotherm revealed a pore size of 27.2 Å, in line with crystallographic analysis, and an apparent surface area of 830 m^2/g (Figure S5 and S6). The molar surface area, 1756 $m^2/mmol$, is also in line with other mesoporous MOFs with similar pore sizes.[10]

Formulating the inorganic SBUs as $[MgH_3(O_2C–)_6]^-$ and considering that there are two inorganic SBUs and one organic SBU (i.e. the three-ligand triad) in each formula unit, **MIT-25** would carry a doubly negative charge: $[Mg_2H_6(TTFTB)_3]^{2-}$..We employed electron paramagnetic resonance (EPR) to elucidate the nature of the charge compensating species. Indeed, **MIT-25** is paramagnetic, and EPR experiments were carried out to further understand the origin and locality of this radical. Continuous-wave (CW) EPR spectra show "powder" rhombic resonance patterns with principal *g* values of 2.014-2.010, 2.0061, 2.002 at the turning points, which are consistent with sulfur based radicals (Figure S8).[11] This was confirmed by collecting spectra at two different frequencies (9 and 34 GHz), which showed that the positions of the resonances were caused by g anisotropy rather than hyperfine coupling. All spectra show more than one set of overlapping resonances, indicating either the presence of more than one radical or the same radical in different chemical environments. We then employed DFT calculations to further substantiate the existence of a single radical per triad. Our model systems, detailed below, revealed that the TTFTB triad could accommodate a single hole, evenly delocalized across the TTF cores. Examination of the spin density further suggested that the observed EPR splitting was unlikely arising from hyperfine coupling, and hence considering these evidences, each organic SBU is best formulated as $(TTFTB)_3^{\bullet+}$.

From elemental analysis, we assign the remaining positive charge to be a hydronium ion, H_3O^+. An analysis of the electron density and electrostatic potential of hydronium-free **MIT-25**, shown in Figure 2, revealed regions of high potential only in the small pore, suggesting that they likely accommodate the hydronium ions. Indeed, although the small pore is narrow, it is sufficiently large to accommodate hydronium and water. Thus, the balanced overall formula for **MIT-25** is best represented as $Mg_2H_6(H_3O)(TTFTB)_3$, where the TTFTB triad caries a –11 charge and the hydronium is likely found in the small pore.

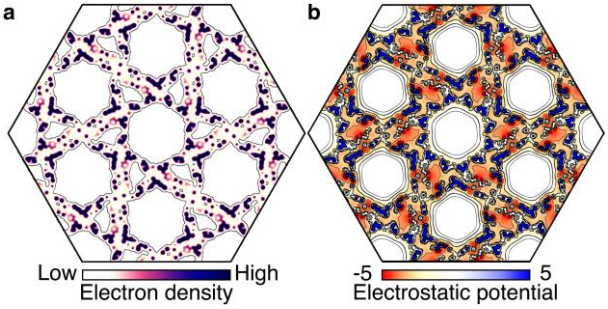

Figure 2. Using a method detailed previously,[12] (a) the computed electron density in both large and small pores rapidly approaches zero in **MIT-25**. (b) The electrostatic potential plateaus in the large pore to a level defined here as zero, while the potential in the small pore is significantly more negative even at the center (red regions).

We conjecture that the radical TTF-based organic SBU is critical in forming the **ssp** net with Mg^{2+}, but is it unique in doing so? To investigate whether other four-connected ligands might give rise to the same net when combined with Mg^{2+} ions, we substituted the TTF core with pyrene, another well-known electron-rich aromatic moiety with a propensity to create interacting aromatic π-systems, and investigated the reactivity of 1,3,6,8-tetrakis(*p*-benzoic acid)pyrene (H_4TBAPy)[13] with various Mg^{2+} precursors. Despite systematically changing reaction conditions including temperature, solvent system, and reagent concentration, we were not able to isolate the **ssp** net with H_4TBAPy. Instead, it exclusively formed $[Mg_3(H_3O)_2(TBAPy)_2(\mu_2\text{-}OH_2)_2(H_2O)_2]\cdot(DMF)_{6.5}(H_2O)(dioxane)_{0.5}$ (**MIT-26**). Crystallizing in space group $P\bar{1}$, **MIT-26** is a two-dimensional MOF wherein neighboring pyrene moieties exhibit short contacts of 3.59 Å, but fail to reproduce the triad organic SBUs that are critical for the formation of the **ssp** net (Figure S9). Thus, despite having similar molecular dimensions and rectangular geometry, H_4TTFTB and H_4TBAPy form vastly different topologies, highlighting the unique role of TTF cores and the organic SBUs in defining overall MOF structure.

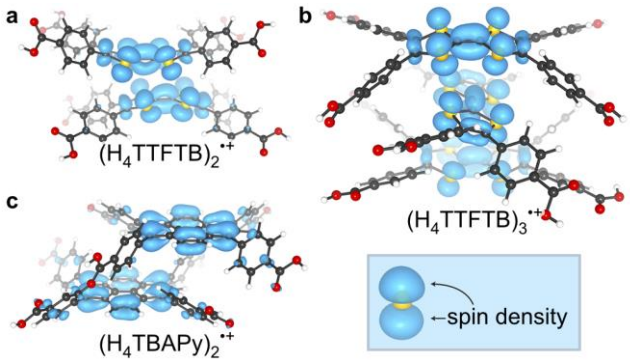

Figure 3. The calculated spin density $(\rho^{\uparrow} - \rho^{\downarrow})$ of (a) $(H_4TTFTB)_2^{\bullet+}$ and (b) $(H_4TTFTB)_3^{\bullet+}$ show full hole delocalization across the TTF core. (c) The $1e^-$ oxidized $(H_4TBAPy)_2^{\bullet+}$ shows similar spin delocalization across the conjugated pyrene core.

Insight into the particular role of TTF, especially as contrasted with pyrene, comes from in-depth computational analysis of the electronic structure of the two ligands, as well as their supramolecular synthons. The calculated electronic structure of H_4TTFTB is similar to that found for TTF itself, with the electrostatic poten-

tial map revealing an electron-rich core centered on the sulfur atoms (Figure S10a). A comparable electronic structure was found for H_4TBAPy, with electron density localized on the pyrene core (Figure S10c). Stacking of two neutral H_4TTFTB or H_4TBAPy is energetically favored, with formation energies of –1.62 and –1.84 kcal/dimer, respectively (Table 1), and both dimers are further stabilized by the presence of a fully delocalized hole, with the formation energy reaching –5.52 and –4.53 kcal/dimer, respectively (Figure 3a,c). While oxidation by one electron is relatively stabilized by increasing the conjugation considered in the system,[14] only TTF has a readily accessible oxidation potential (E = 0.34 V vs. Ag/AgCl in MeCN)[15], whereas TBAPy remains neutral under similar synthetic conditions (E = 1.16 V vs. SCE in MeCN).[16] In summary, we would not expect the H_4TBAPy to oxidize in air to form the hypothetical dimer presented in Figure 3c.

The addition of a second neutral H_4TTFTB ligand to a $(H_4TTFTB)_2^{\bullet+}$ dimer provides significant further stabilization to the $(H_4TTFTB)_3^{\bullet+}$ trimer (–13.73 kcal/trimer), and the associated electronic hole is fully delocalized over all three TTF cores (Figure 3b). The geometry of the TTF core serves as a metric for the extent of oxidation. Delocalization of the hole in each $(TTFTB)_3^{\bullet+}$ SBU in **MIT-25** is indeed supported by X-ray crystallographic analysis, from examination of the C–S and central C=C bond lengths, which vary by only 0.0015 Å and 0.007 Å, respectively (Table S2). This indicates that all three TTF units in a single triad carry equivalent (partial) oxidation states.[17]

Table 1. Stacking formation energies for H_4TTFTB and H_4TBAPy as calculated from density functional theory.

	Formation energy (kcal/mol)
$(H_4TTFTB)_2$	–1.62
$(H_4TTFTB)_2^{\bullet+}$	–5.52
$(H_4TTFTB)_3^{\bullet+}$	–13.73
$(H_4TBAPy)_2$	–1.84
$(H_4TBAPy)_2^{\bullet+}$	–4.53

Although the formation of π-interacting motifs provides overall stabilization, as seen with **MIT-26** and numerous other examples,[2] these studies emphasize the importance of accessing oxidized species as well as delocalizing the holes to stabilize organic SBUs. These principles are illustrated in **MIT-25**, whose unique mesoporous structure and new topology only arise because of the organic SBU. The formation of π-stacked organic SBUs by the deliberate introduction of holes may serve as a general strategy for the formation of materials with new topologies.

ASSOCIATED CONTENT

Supporting Information

Detailed experimental procedures and computational details; single crystal and powder X-ray diffraction data, N_2 adsorption isotherms, TGA and EPR. This material is available free of charge via the Internet at http://pubs.acs.org.

AUTHOR INFORMATION

Corresponding Author

mdinca@mit.edu

Notes

The authors declare no competing financial interests.

ACKNOWLEDGMENT

This work was supported as part of the Center for Excitonics, an Energy Frontier Research Center funded by the US Department of Energy, Office of Science, Office of Basic Energy Sciences, under award no. DE-SC0001088 (MIT). M.D. gratefully acknowledges early career support from the Sloan Foundation, the Research Corporation for Science Advancement (Cottrell Scholar), and the Dreyfus Foundation. S.S.P. is partially supported by a National Science Foundation Graduate Research Fellowship (Award No. 1122374). S.S.P. thanks to M. Korzyński for providing H_4TBAPy. A.J.F. is supported by Bruker. All EPR experiments were carried out at the EPSRC National EPR Facility and Service, University of Manchester, UK. A.W. is supported by the ERC (grant no. 277757). We thank Dr. P. Müller and Dr. J. Becker for assistance with crystallography and Prof. O. Yaghi for valuable discussions. Computational work was enabled by access to XSEDE, which is supported by NSF grant number ACI-1053575.

REFERENCES

(1) (a) Yaghi, O. M.; O'Keeffe, M.; Ockwig, N. W.; Chae, H. K.; Eddaoudi, M.; Kim, J. *Nature* **2003**, *423*, 705. (b) Nouar, F.; Eubank, J. F.; Bousquet, T.; Wojtas, L.; Zaworotko, M. J.; Eddaoudi, M. *J. Am. Chem. Soc.* **2008**, *130*, 1833. (c) Cairns, A. J.; Perman, J. A.; Wojtas, L.; Kravtsov, V. C.; Alkordi, M. H.; Eddaoudi, M.; Zaworotko, M. J. *J. Am. Chem. Soc.* **2008**, *130*, 1560. (d) Tranchemontagne, D. J.; Mendoza-Cortés, J. L.; O'Keeffe, M.; Yaghi, O. M. *Chem. Soc. Rev.* **2009,** *38*, 1257. (e) Yaghi, O. M.; Li, Q. *MRS Bull.* **2009**, *34*, 682. (f) Perry IV, J. J.; Perman, J. A.; Zaworotko, M. J. *Chem. Soc. Rev.* **2009**, *38*, 1400. (g) Mellot-Draznieks, C.; Cheetham, A. K. *Nat. Chem.* **2017**, *9*, 6.

(2) (a) Amabilino, D. B.; Stoddart, J. F. *Chem. Rev.* **1995**, *95*, 2725. (b) Claessens C. G.; Stoddart, J. F. *J. Phys. Org. Chem.* **1997**, *10*, 254. (c) Chen, B.; Eddaoudi, M.; Hyde, S. T.; O'Keeffe, M.; Yaghi, O. M. *Science* **2001**, *291*, 1021. (d) Dincă, M.; Dailly, A.; Tsay, C.; Long, J. R. Inorg. Chem. **2008**, *47*, 11. (e) Reger, D. L.; Horger, J.; Smith, M. D.; Long, G. J. *Chem. Commun.* **2009**, *41*, 6219. (f) Nakano, T. *Polym. J.* **2010**, *42*, 103. (g) Chen, T.-H.; Popov, I.; Miljanić, O. S. *Chem. Eur. J.* **2016**, *22*, 1.

(3) (a) Govers, H. A. J.; de Kruif, C. G. *Acta Cryst.* **1980**, *A36*, 428. (b) Hunter, C. A.; Sanders, J. K. M. *J. Am. Chem. Soc.* **1990**, *112*, 5525. (c) Martinez, C. R.; Iverson, B. L. *Chem Sci.* **2012**, *3*, 2191.

(4) (a) Kollman, P. A.; Allen, L. C. *J. Chem. Phys.*, **1969**, *51*, 3286. (b) Smith, J. D.; Cappa, C. D.; Wilson, K. R.; Messer, B. M.; Cohen, R. C.; Saykally, R. J. *Science*, **2004**, *306*, 851.

(5) (a) Rodgers, M. T.; Armentrout, P. B. *Mass Spec. Rev.* **2000**, *19*, 215. (b) Armentrout, P. B., Halle, L. F., Beauchamp, J. L. *J. Am. Chem. Soc.*, **1981**, *103*, 6501.

(6) (a) Narayan, T. C.; Miyakai, T.; Seki, S.; Dincă, M. *J. Am. Chem. Soc.* **2012**, *134*, 12932-12935. (b) Park, S. S.; Hontz, E. R.; Sun, L.; Hendon, C. H.; Walsh, A.; Van Voorhis, T.; Dincă, M. *J. Am. Chem. Soc.* **2015**, *137*, 1774.

(7) Barrett, E. P.; Joyner, L. G.; Halenda, P. P. *J. Am. Chem. Soc.* **1951**, *73*, 373.

(8) Kruk, M.; Jaroniec, M.; Sayari, A. *Langmuir* **1997**, *13*, 6267.

(9) Brunauer, S.; Emmett, P. H.; Teller, E. *J. Am. Chem. Soc.* **1938**, *60*, 309.

(10) Deng, H.; Grunder, S.; Cordova, K. E.; Valente, C.; Furukawa, H.; Hmadeh, M.; Gándara, F.; Whalley, A. C.; Liu, Z.; Asahina, S.; Kazumori, H.; O'Keeffe, M.; Terasaki, O.; Stoddart, J. F.; Yaghi, O. M. *Science* **2012**, *336*, 1018.

(11) Chatgilialoglu, C.; Asmus, K.-D. *Sulfur-Centered Reactive Intermediates in Chemistry and Biology;* Springer Science & Business Media: New York, 2013.

(12) (a) Walsh, A.; Butler, K. T.; Hendon, C. H. *MRS Bull.* **2016**, *41*, 870; Codes available from goo.gl/O1ItdU (b) Butler, K. T., Hendon, C. H., Walsh, A. *J. Am. Chem. Soc.* **2014**, 136, 2703.

(13) Stylianou, K. C.; Heck, R.; Chong, S. Y.; Bacsa, J.; Jones, J. T. A.; Khimyak, Y. Z.; Bradshaw, D.; Rosseinsky, M. J. *J. Am. Chem. Soc.* **2010**, *132*, 4119.

(14) Hendon, C. H.; Carbery, D. R.; Walsh, A. *Chem. Sci.* **2014**, *5*, 1390.

(15) Bendikov, M.; Wudl, F.; Perepichka, D. F. *Chem. Rev.* **2004**, *104*, 4891.
(16) Murov, S. L.; Carmichael, I.; Hug, G. L. *Handbook of Photochemistry*; Marcel Dekker: New York, 1993.
(17) (a) Cooper, W. F.; Kenny, N. C.; Edmonds, J. W.; Nagel, A.; Wudl, F.; Coppens, P. *J. Chem. Soc. D* **1971**, *16*, 889. (b) Kistenmacher, T. J.; Phillips, T. E.; Cowan, D. O. *Acta Cryst.* **1974**, *B30*, 763. (c) Clemente, D. A.; Marzotto, A. *J. Mater. Chem.* **1996**, *6*, 941.